NASA DEVELOP National Program

Southeastern Idaho Water Resources II

Utilizing NASA Earth Observations to Identify Existing Surface Water Features and Improve Water Management and Resource Allocation in Southeastern Idaho

DEVELOP Technical Report

Rough Draft – February 16, 2017

Cody O'Dale (Project Lead)
Austin Counts
Brooke Colley
Claire Haupt
Paul Bushman
Courtney Ohr

Keith Weber, GIS Training and Research Center at Idaho State University (Lead Science Advisor)
Mark Carroll, NASA Goddard Space Flight Center (Science Advisor)
Charles Peterson, Idaho State University (Science Advisor)

Previous Contributors:
Traci Olson
Dylan Thomas
Caitlin Toner

1. Abstract

Understanding water dynamics in southeast Idaho is critical to planning and improving water management practices. Partner organizations that focus on water resource management, such as the Bureau of Land Management (BLM) and Idaho Department of Water Resources (IDWR), currently use the National Hydrography Dataset and expert knowledge to identify water bodies. This approach has been insufficient to meet all their needs because these datasets may not always reflect current ground conditions. This poses a risk for officials at the BLM and IDWR that could lead to ineffective use of their resources and inefficient management practices. To counter this shortcoming, this study was undertaken using NASA Earth observations within Google Earth Engine (GEE) and Esri's ArcGIS to create a capability that would allow end-users to better identify and track water bodies within their management area. Known as the Surface Water Indicator Model (SWIM), this tool incorporated Landsat 8 imagery, Sentinel-2 imagery, multiple derived water indices, and topographic data into a Support Vector Machine (SVM) classifier. This study combines these data indices into a single tool to create an accurate surface water indicator. The resulting SWIM tool was created in both GEE and Esri's ArcGIS to allow end-users their choice of platform. The SWIM tool will provide natural resource managers with current and seasonal surface water indication and more accurate data for land management.

Keywords
Remote sensing, surface water, Support Vector Machine, Sentinel-2, Landsat 8 OLI, water index, water resources, SWIM, Google Earth Engine.

2. Introduction

2.1 Background Information

Previous research has identified surface water bodies through the use of water indices (McFeeters, 2013) or a classification algorithm (Wright & Gallant, 2007), but most have not combined the two methods. Often, any one of these methods alone, will incorrectly classify mountain shadows (Jin et al. 2013), urban asphalt (Feyisa et al. 2014), basaltic lava flows, or dark vegetation, (Jawak et al. 2015) as water. This study combines multiple water indices, as well as a classification algorithm into a single tool, to create a more accurate surface water indicator. This indicator expands upon Landsat's extensive record of earth observation imagery, while also leveraging higher spatial resolution Sentinel-2 imagery as well. The scope of this study area spans from the east edge of Craters of the Moon National Monument to Bear Lake, Idaho. The landscape hosts abundant ecological diversity including large areas of basaltic lava flows, forested mountains, marshlands, reservoirs, ponds, rivers, and large

Figure 1. Study area extent (red) of Southeastern Idaho Water Resources project.

areas of sporadic vegetation with bare soil. The tool produced during this study used imagery from 2016 for its initial testing, but was designed for broader partner use in seasonal water monitoring for surface water extent. This study developed the Surface Water Indication Model (SWIM) tool, along with a database to

1

identify current seasonal variability of surface water occurrence.

2.2 Project Partners & Objectives

Partners for this project included the Bureau of Land Management (BLM) - Pocatello Field Office, the Idaho Department of Water Resources (IDWR), and the NASA RECOVER Science Team at Idaho State University's GIS Training and Research Center (ISU's GIS TReC). Currently, end-user agencies (BLM and IDWR), are responsible for the management of surface water bodies to meet both urban and rural water needs, and to manage natural resources and wildlife habitat in southeast Idaho. Neither of our end-users are familiar with using satellite data to identify surface water features; instead they rely on spatial and non-spatial legacy data to identify areas that require special management practices. Therefore, satellite data was explored as an alternative source of information.

2.3 Support Vector Machine (SVM) Classifier

A Support Vector Machine (SVM) classifier is a supervised machine-learning algorithm that helps describe, categorize, and generalize a particular dataset. This algorithm was originally developed for pattern recognition. It's commonly used for image classification because of its strong theoretical foundation and experienced success (Cafarella et al. 2008). SVM aims to find the uniform convergence, or the "true" mean of spectral signatures of the labeled training points, creating a division line or classifier. The largest gap being between the classifier and the training data, is called trick optimization (Figure 2A). When the unlabeled pixel signatures are plotted on the chart, they will fall on either side of these class lines giving the predicted classification. SVM can also create hyperplanes when signatures become too complex and there is no way to create a simple line for the mean of a signature class (Figure 2B). Creating a hyperplane involves kernelling or transforming the data so that it becomes more uniform, allowing the hyperplane to be drawn into three dimensions (Burges, 1998). Normally, using SVM results in decreased computation time and increased memory requirements. However, a parallel SVM algorithm was implemented within Google Earth Engine (GEE) due to its memory capacity, which bypassed these downfalls. The ArcMap version currently does not have this capability, but users can define the number of processors used for the SVM computation. This does help negate some of the computation complexities.
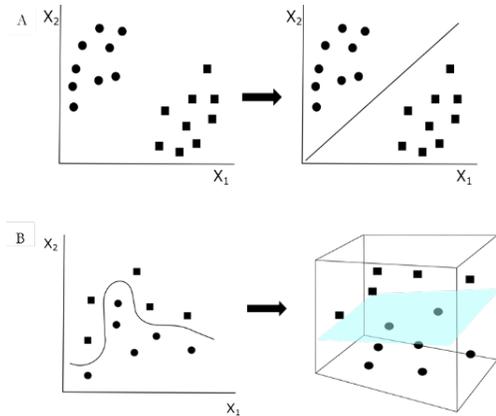
Figure 2. Classifying with SVM where two classes (shown as circles for water and squares for non-water) are known to be present. A) The mean is shown with the line and has been trick optimized so that the distances from the closest point in each of the two groups will be farthest away. Wherever the unlabeled signatures fall will decide if it is water or not water. B) When the labeled training data has too much variation a transformation is implemented and a hyperplane (shown in blue) is created.

2.4 Hosting Platforms: Google Earth Engine (GEE) & Esri ArcGIS

To increase SWIM usability, two platforms were used. GEE is a cloud-based, geospatial platform that processes satellite imagery and other global observation data. This platform integrates a variety of available public datasets, and uses Google's server capacity to perform numerous geospatial processes. Additionally, work done on GEE can be integrated into a publicly available console and shared with other users. The Esri software provides multiple platforms for visualizing, analyzing, exploring spatial relationships, patterns, and trends. While this software is tailored toward vector data rather than raster processing, the software is widely used; therefore, making it ideal for disseminating the SWIM tool.

3. Methodology

This SWIM tool was created in both GEE using JavaScript (SWIM-GEE) and Esri's ArcGIS using python scripting (SWIM-ArcGIS). This tool consists of four types of inputs: water indices, vegetation imagery, topographic layers, and secondary variables. These inputs were derived from Landsat 8 Operational Land

Imager (OLI) (US Geological Service, 2014) or Sentinel-2 multi-spectral instrument (MSI) imagery, along with Shuttle Radar Topography Mission (SRTM) data (NASA JPL., 2016). Both SWIM-GEE and SWIM-ArcGIS, used surface reflectance values to calculate water indices, the same training points, and SVM classifier. Training points used for both platforms were created within the GEE platform, using 2016 Google imagery. Over 40 training polygons, covering a minimum of 10 pixels each, were specified for each of the five classes: basalt, open water, dark vegetation, urban, and sporadic vegetation and/or bare soil. The input layers and training points were used within a supervised classifier called a Support Vector Machine (SVM). This distinguished commonalities of each class, and labeled such signatures as one of the five classes. They were then classified as water body or non-water features.

The SWIM-ArcGIS platform is similar to the SWIM-GEE platform. Nonetheless, it differs in its final calculations of the end product because SWIM-ArcGIS uses the Boolean sum of the water indices. The SVM classifier was used on each of the water indices to give a value of 1-water or 0-non-water; rather than all of the inputs at one time. Those raster layers were then totaled so that pixels were given a value of 0-5, producing a single raster. A value of 0 indicated the pixel was identified as non-water across all of the classified water indices, while 1 specified that one of the five classified water indices categorized the pixel as a water feature. A value of 2 designated that two of the five classified water indices indicated water and so forth. This provided a confidence rating for the ArcGIS results. For instance, if a pixel was classified as 5, then there was high likelihood that surface water was correctly identified for that pixel. A value of 1 meant that lower confidence water actually existed in that location. Though the same initial methods were implemented in each platform, a degree of confidence was not available from the SWIM-GEE result. Instead, a classified map with all five classes was produced. After the SWIM tool was created and tailored to run with 30 and 10 meter resolution imagery, it was run across a time series of imagery throughout the 2015 and 2016 water years to help differentiate intermittent and perennial water bodies.
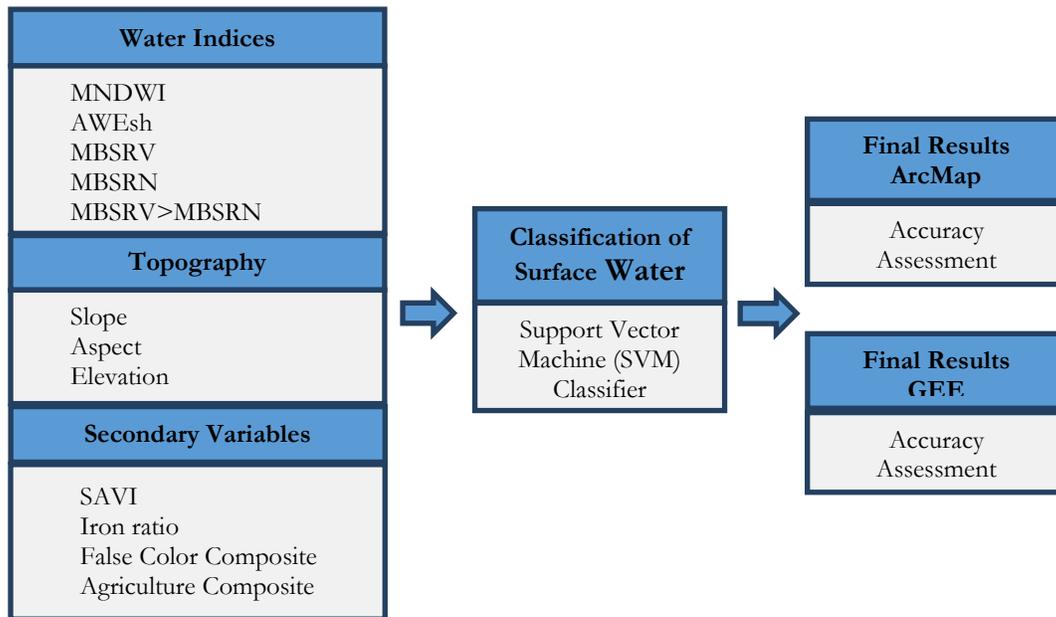
Figure 3. The SWIM tool consisted of three components- water indices (Modification of Normalized Difference Water Index (MNDWI), multi-band spectral relationship near infrared (MBSRN), multi-band spectral relationship visible (MBSRV), Automated Water Extent with Shadow (AWEsh)), topography, and secondary variables (soil adjusted vegetation index (SAVI), the iron ratio, and thermal band 10) derived from Landsat 8 OLI/TIRS imagery and SRTM data. These three components were then added to a classifier within two separate platforms in order to identify surface water bodies, these results then underwent validation.

3.1 Data Acquisition

Two types of data, topography and multi-spectral imagery, were used in the SWIM tool. The multi-spectral data was provided by Landsat 8 OLI & TIRS (paths 39, 38 & rows 30, 31) and by Sentinel-2 MSI. The surface reflectance was recorded at 30 meter and 100 meter spatial resolution for Landsat, and 10 meter spatial resolution for Sentinel. Imagery was collected between June of 2016 and September of 2016. A path refers to how a satellite collects data by running north to south, and a row is the east to west position of each image (Irons, 2016). For SWIM-GEE, Landsat scenes were used from the available USGS top of the atmosphere (TOA) reflectance repository in GEE. For SWIM-ArcGIS, Landsat scenes were downloaded from USGS Earth Explorer for use in ArcGIS. The topography data came from the Shuttle Radar Topography Mission (SRTM) digital elevation dataset at 10 and 30 meter spatial resolution. This was found in the GEE repository for SWIM-GEE, or was downloaded from the US Department of Agriculture geospatial data gateway being used in ArcGIS for the SWIM-ArcGIS tool. Finally, field verification points will be provided by BLM partners after the summer of 2017.

3.2 Data Processing & Analysis

3.2.1 Water Indices

Water indices were incorporated into the classification as a means to better locate surface water within the study area. Different types of water indices exist and each have some margin of error. For example, in some instances irrigated croplands may be falsely identified as similar to riparian environment (Donchyts et al. 2016). To reduce error, several water indices were used in this classification.

Modified Normalized Difference Water Index

The modified normalized difference water index (MNDWI) differs from the original normalized difference water index (NDWI) as it was derived from the green and middle shortwave infrared (SWIR1) bands rather than green and near infrared (NIR) bands. The NDWI often overestimates the amount of water due to spectral noise caused by vegetation and soil. The MNDWI is able to remove the signal of vegetation and soil, while more effectively detecting open water bodies relative to NDWI (Xu, 2006). Similar to a normal NDWI, the MNDWI identifies changes in liquid water content of vegetation canopies. MNDWI values range from -1.0 to 1.0 and the index maximizes the reflectance values of water and also minimizes vegetation and soil values. As water is rarely ever crystal clear, MNDWI is highly sensitive to fluctuations in water turbidity, yet identifies more water signatures than NDWI. MNDWI is more vulnerable than NDWI to false positives normally caused shadows due to the hills and clouds (Donchyts et al. 2016).
.

$$\text{A.} \quad \text{NDWI} = \frac{\varrho_{green} - \varrho_{NIR}}{\varrho_{green} + \varrho_{NIR}}$$

$$\text{B.} \quad \text{MNDWI} = \frac{\varrho_{green} - \varrho_{SWIR1}}{\varrho_{green} + \varrho_{SWIR1}}$$

Equation 1. NDWI (A) and MNDWI (B) equation where ϱ is the reflectance value of the spectral bands (i.e. green).

Multi-band Spectral Relationships

The multi-band spectral relationship near infrared (MBSRN) index is calculated by combining the NIR and SWIR1 bands. All while the multi-band spectral relationship visible (MBSRV) index is derived from the green and red bands. The MBSRN band combination was used because these spectral ranges are absorbed by water, making water features appear dark. When the MBSRV value is greater than the MBSRN value, the pixel is more likely to contain more water than vegetation (Jones & Starbuck, 2015). Thus, creating a threshold. These calculations comprise three of the bands in the SWIM stack.

$$\text{A.} \quad \text{MBSRV} = \varrho_{green} + \varrho_{red}$$

$$\text{B.} \quad \text{MBSRN} = \varrho_{NIR} + \varrho_{SWIR1}$$

$$\text{C.} \quad \text{MBSRthreshold} = \text{MBSRV} > \text{MBSRN}$$

Equation 2 Calculations for MBSRV (A), MBSRN (B) and the threshold between the MBSR values (C) where ϱ is the reflectance value of the spectral bands (i.e. green).

Automated Water Extent with Shadow (AWE_sh)

Consisting of the Blue, Green, and SWIR 2 bands, while including MBSRN (Equations *2*B), this equation is a further improvement on the distinction of shadow areas and dark surfaces. AWE$_{sh}$ builds upon pre-existing water indices using a multi-band index rather than relying on dual-band ratios or single-band thresholding. Through band differencing, addition, and applying varying coefficients, the index's primary goal is to maximize separation between water and non-water dark pixels (Feyisa et al. 2014). The application of AWE$_{sh}$ in this study was intended for when shadows present sources of accuracy loss.

$$\text{AWE}_{sh} = \varrho_{blue} + \left(2.5\varrho_{green}\right) + \left(\text{-}1.5(\varrho_{NIR} + \varrho_{SWIR1})\right) + \left(\text{-}0.25\varrho_{SWIR2}\right)$$

Equation 3 Calculation for AWE$_{sh}$ index, where ϱ is the reflectance value of the spectral bands (i.e. green)

3.2.3 Topographic variables

A 30 meter digital surface model (DSM) was chosen to match the 30 meter spatial resolution of Landsat 8 OLI data; while the 10 meter DSM was chosen to be use with Sentinel-2 MSI data. The DSM were used in SWIM to add layers of elevation, slope, and aspect. These topography layers were included to help separate possible false positives on steep slopes or dry hill faces.

3.2.4 Agriculture

When choosing land cover type for the classes, it was difficult to determine a class type for agriculture. Crops that were in the process of rotation could have been freshly watered or recently harvested when the satellite acquired the imagery. Originally, agricultural crops would sometimes be labeled as dark vegetation or mixed water, and the dead and dry crops would be mislabeled as urban or bare soil. This was counteracted using several vegetation detection methods. A false color image was created to better differentiate variability in crop areas. Likewise, an agriculture band combination within Sentinel-2 was used to detect areas that were most likely to be crops or regenerating agricultural land.

3.2.5 Secondary Variables

Soil Adjusted Vegetation Index (SAVI)

The Normalized Difference Vegetation Index (NDVI) was considered as an indicator of live green vegetation within a pixel as it might indicate a water source. MSAVI was considered, but due to short duration of research time, we weren't able to effectively integrate the code. The SAVI equation builds upon the NDVI equation by introducing a constant to adjust for soil reflectance. That constant can be chosen based on the type of soil to vegetation mixtures that one would expect in a given study site, ranging from 0 for dense vegetation, to 1 for sparse vegetation with more bare soil than green vegetation (Huete, 1988). In this project the constant 0.5 was used to represent an even mixture of bare soil to vegetation. The study area has a large amount of bare soil with sporadic vegetation, therefore, vegetation indices would likely increase model proficiency.

$$\text{A.} \quad \text{NDVI} = \frac{\varrho_{NIR} - \varrho_{red}}{\varrho_{NIR} + \varrho_{red}}$$

$$\text{B.} \quad \text{SAVI} = \left(\frac{\varrho_{NIR} - \varrho_{red}}{\varrho_{NIR} + \varrho_{red} + L}\right)(1+L)$$

Equation 4 Calculations for NDVI (A) and for SAVI (B), where ϱ is the reflectance value of the spectral bands (i.e. green) and L represents a constant known as the soil brightness correction factor.

Iron Ratio & Thermal Band

Two factors were used to distinguish water from basalt. Basalt is a feature that is commonly misidentified as

water. First, basalt was designated as one of the training classes in the SVM classifier. Second, the ratio of the red band over the green band assists in distinguishing ferric iron (Kalinowski & Oliver, 2004). Within SWIM, this is often referred to as the iron ratio.

$$\text{ferric iron} = \frac{\varrho_{\text{red}}}{\varrho_{\text{green}}}$$

Equation 5 Calculation for the iron ratio, where ϱ is the reflectance value of the spectral bands (i.e. green).

3.2.1 Error Assesment

To test the level of accuracy of the final classification results, an error matrix was used. The classifier was trained with a randomly selected subset of 60 percent of the training points. The error matrix in GEE used the remaining 40 percent of the training points as validation sites. This process was run three times with a new 60/40 randomization each time. The average overall accuracy of the three error matrices was reported in GEE's console. The error analysis process was repeated in ArcGIS for comparison. Within ArcGIS 150, random points were generated so that 30 points fell inside each of the five classes. These points were then compared to aerial imagery from the 2015 National Agriculture Imagery Program (NAIP).

4. Results & Discussion

Advanced users have the ability to customize SWIM within GEE, while Esri's ArcMap provides accessibility for users who are already familiar with Esri software. However, GEE is limited by its script-based interface while Esri provides a more common Graphical User Interface (GUI). Gee requires users to make JavaScript based edits in order to use SWIM. A GUI may be more intuitive, but a script based interface enables a higher degree of modification. The Esri suite is tailored toward vector data rather than raster processing; although the software is widely used and therefore ideal for disseminating the SWIM tool. The Esri ArcMap software allows production of a GUI; providing a more intuitive interface for users unfamiliar with programming technology. Unfortunately, the overall ability of the SWIM tool varied from the GEE developed SWIM tool. This was due to the available classifiers and computation performance differences across the two platforms. The overall accuracy of the SWIM-GEE platform model was 68% (Table 1) and 97% (Table 2) when calculated in GEE and ArcMap, respectively. The independent validation created within ArcGIS reported an accuracy of 80% for correctly identifying water. SWIM-ArcGIS had an overall accuracy of 96% and due to differences in SWIM methods across platforms, this should be considered the same accuracy for overall water identification.

Intermittent water bodies were successfully identified using two time-steps for 2016 imagery from Sentinel-2 and four time-steps for 2016 imagery from Landsat 8. The spatial extent of the intermittent streams were noticeably dependent on how the training and validation points were split. For that reason, results for intermittent streams included a confidence rating (Figure 5). When results from the SWIM-GEE (Figure 4a) and SWIM-ArcGIS (Figure 4b) platforms were compared, they agreed well on all "non-water" classes, but there was some variation regarding water body detection (Figure 6). Spatial resolution played a large role in determining if river connectivity existed, and also in defining the spatial boundaries of the surface water bodies (Figure 7). In addition, there were some discrepancies of detecting water that may be due to two reasons: 1) differences of when the Landsat 8 acquired imagery and when Sentinel-2 collected imagery, and 2) differences between sensor bandwidth ranges and the ration of signal to noise as spatial resolution decreases (Figure 8).

4.1 Accuracy

The overall high accuracy of the GEE validation may be due to the high number of validation points, 11,719 pixels, while the ArcGIS independent validation consisted of only 150 pixels. The GEE algorithm for performing these validation calculations is not available for public review and therefore could be redundantly included training points in the validation assessment. An 80% accuracy for water indicates the model was successful in identifying surface water bodies. The overall accuracy was low due to mis-identifying non-water classes (Table 1). This is not concerning, because the mis-identified pixels were not regularly confused with water. It is also expected that non-water classes would have trouble during classification; since the inputs for the SWIM tool consisted of water indices and not variables specifically chosen to help identify non-water classes.

Table 1. Independent test of GEE-SWIM using stratified random sampling to determine validation points and NAIP 2015 imagery to determine accuracy.

Classes	Basalt	Open Water	Dark Vegetation	Urban	Bare Soil/ Sporadic Vegetation	User Accuracy
Basalt	17	2	3	5	1	61%
Open Water	3	24	0	3	0	80%
Dark Vegetation	0	2	21	0	2	84%
Urban	0	2	0	16	3	76%
Bare Soil/Sporadic Vegetation	10	0	6	6	24	52%
Producer Accuracy	57%	80%	70%	53%	80%	

Table 2. Error matrix for overall accuracy of the SWIM tool when using the GEE platform. Each class was verified to determine the likelihood of the model detecting that particular feature. The average accuracy of detecting water was 83%.

Classes	Basalt	Open Water	Dark Vegetation	Urban	Bare Soil/ Sporadic Vegetation	Accuracy
Basalt	1400	4	4	1	3	99%
Open Water	0	2631	0	0	0	100%
Dark Vegetation	0	0	1252	1	220	85%
Urban	0	1	9	549	0	98%
Bare Soil/Sporadic Vegetation	54	0	0	1	5589	99%
Accuracy	96%	100%	99%	99%	96%	

4.3 Comparison of platform performance in SWIM

Figure 4b shows those pixels that have at least a level two confidence of water displayed in blue, (the reader may recall, this means at least two water indices identified the pixel as water). A visual comparison illustrated that the SWIM-ArcGIS map matches the SWIM-GEE map for nearly all major water bodies. However, some places such as the northern part of the American Falls Reservoir do not appear in SWIM-ArcGIS (Figure 4b), while these features do show in SWIM-GEE results (Figure 4a).
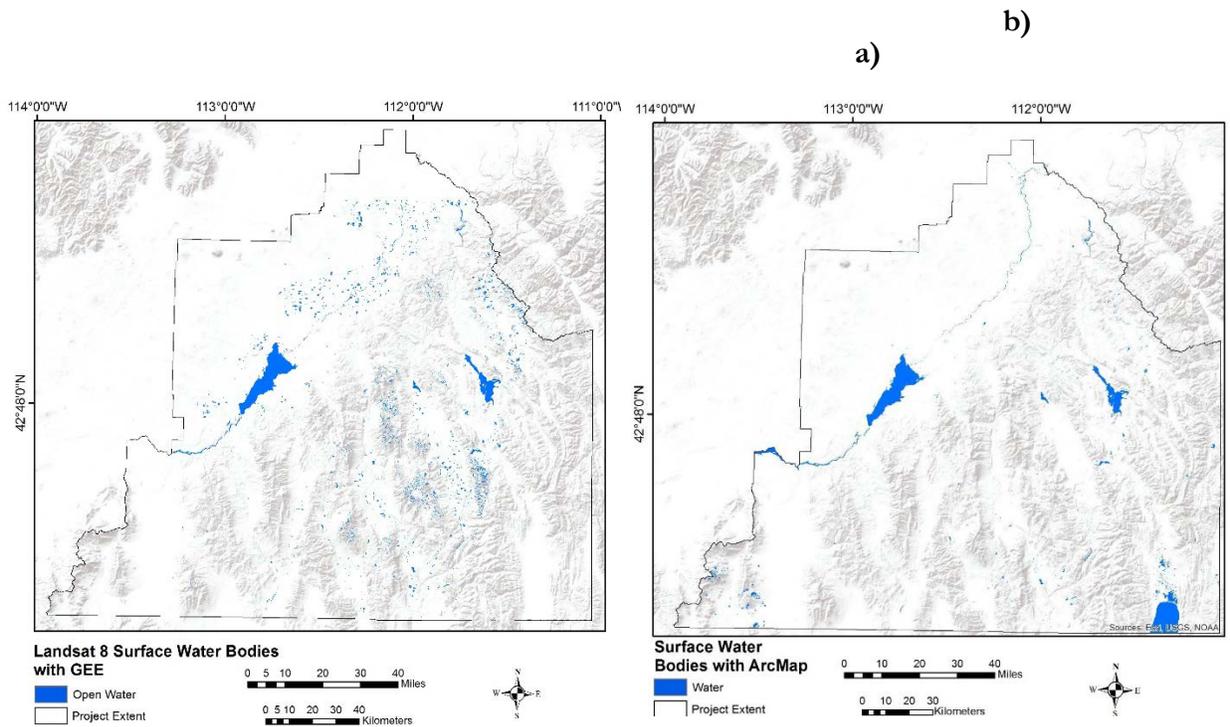
Figure 4. Overview of the study area with the water bodies identified by the SWIM-GEE tool while using JavaScript in GEE. b) An overview of the study area and the water bodies the SWIM-ArcGIS tool identified using Python in ArcGIS

Most of the disagreement between the ArcGIS and GEE platform were due to SWIM-ArcGIS classifying pixels as "non-water" when SWIM-GEE classified the pixel as "water". This accounted for 3.48% of the total 4.95% disagreement (Table 3). This may have been caused by a combination of factors. The classifier, even though SVM was the chosen classifier in both platforms, may have operated differently within each platform. In addition, the last steps in SWIM-ArcGIS converted all results into a binary "water" versus "non-water" layer.
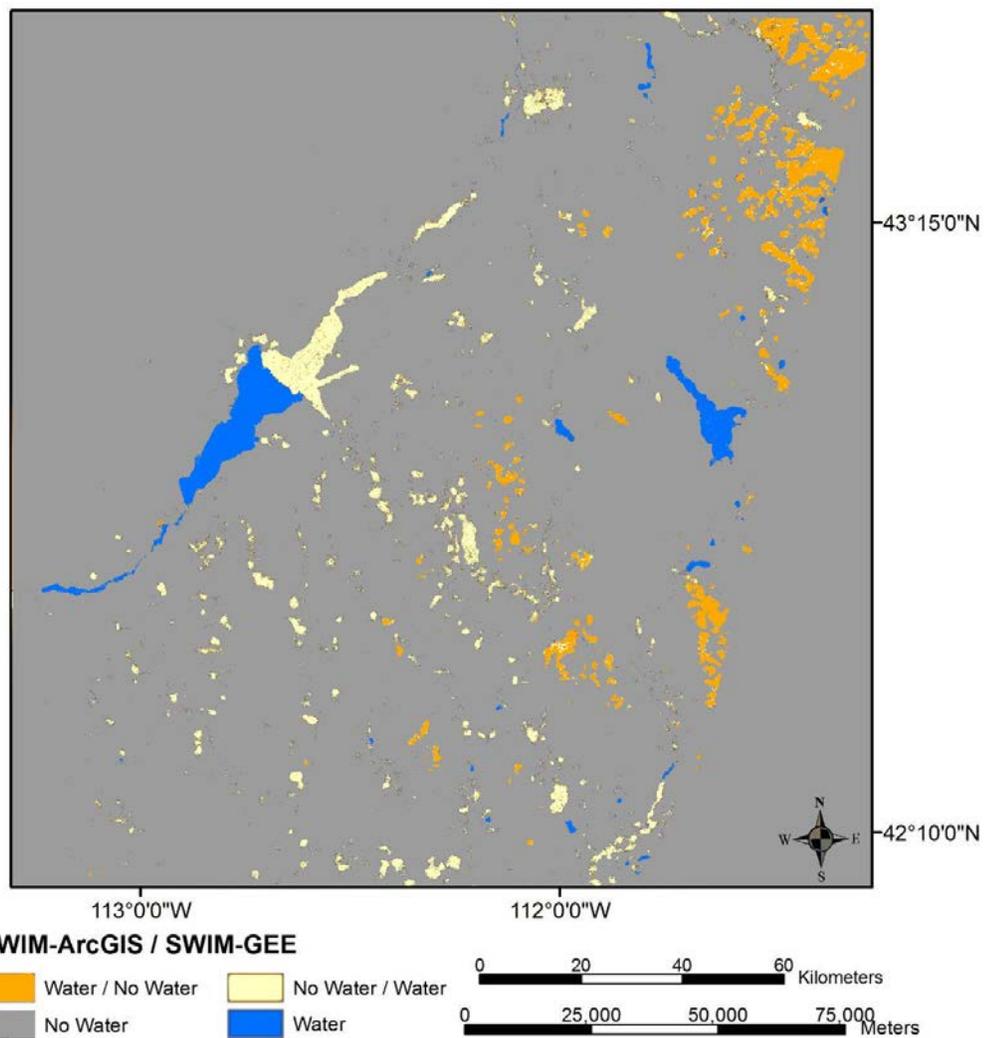
Figure 5. SWIM-ArcGIS's results produced in ArcMap were compared to the SWIM-GEE product with an agriculture mask applied. The figure displays pixels that were classified as water by the SWIM-ArcGIS and non-water as SWIM-GEE in red; orange shows pixels that SWIM -ArcGIS classified non-water and SWIM-GEE classified as water pixels; areas where both models classified pixels as non-water are shown in gray and water in blue.

Table 3. Summary of the areas (km²) compared between SWIM Platforms

	Area	
ArcGIS / GEE	KM²	Percent
No Water	2,5095	94%
Water	333	1%
No Water / Water	930	4%
Water / No Water	394	1%
Total Agreement	2,5428	95%

9

Total Disagreement	1,325	5%

4.2 Identifying Intermittent Water Bodies
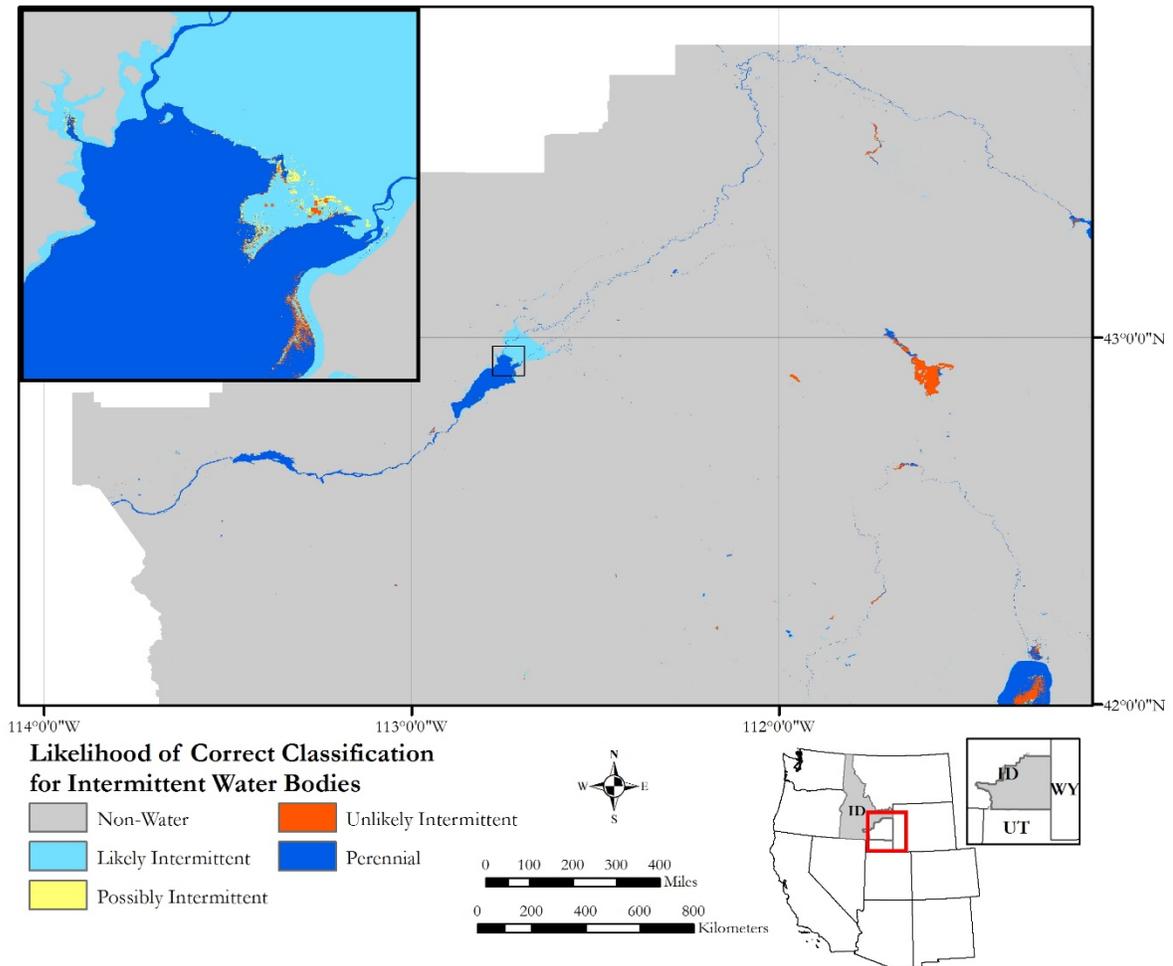
Figure 6. Likelihood of SWIM tool correctly identifying intermittent water bodies.

In Figure 5, pixels identified as intermittent between July 06, 2016 and August 24, 2016 were given

Sentinel-2 not only provided better resolution imagery, but allowed for more accurate classifications of dry and wet season images. These images were overlaid together to create seasonality maps indicating the presence of perennial and intermittent water bodies. After creating the seasonality layers, these layers were used to create a likelihood map to more precisely show the presence of each water body type (Figure 5). Intermittent water bodies were identified as likely intermittent if there were no change between the July 26 and August 24, 2016 imagery for all three time periods used in the classifier. Possibly intermittent water bodies were those that did not consistently detect an intermittent water body across all three classification time periods, while unlikely intermittent describes those results where water was identified during only one of the three time periods analyzed. There were only a few classifications that created an unlikely intermittent water body and these were likely caused by shallow water bodies or those with increased sedimentation which

may have caused confusion with the signatures of the wet soil, exposed substrate, and water classes.

4.4 GEE-SWIM comparison of resolutions across Landsat 8 and Sentinel-2

For the July 2016 sensor comparison (Figure 7) we found strong agreement between non-water features. The large perennial surface water bodies appear constant across seasons. However, there was substantial disagreement water body edges between Sentinel-2 and Landsat 8. Figure 7 shows Sentinel-2 water vs. Landsat 8 non-water features especially in the inset imagery. Landsat 8 water vs. Sentenel-2 non-water seems to be more sporadic and shows water further way from large water bodies. This class is less prevalent during the wet season (Figure 8) than the dry season (Figure 7). The inset map of Figure 7 and Figure 8 shows that the disagreement of non-water / water (Sentinel-2 / Landsat) in the dry season is reversed to water / non-water (Sentinel-2 / Landsat) during the wet season. In general resolution
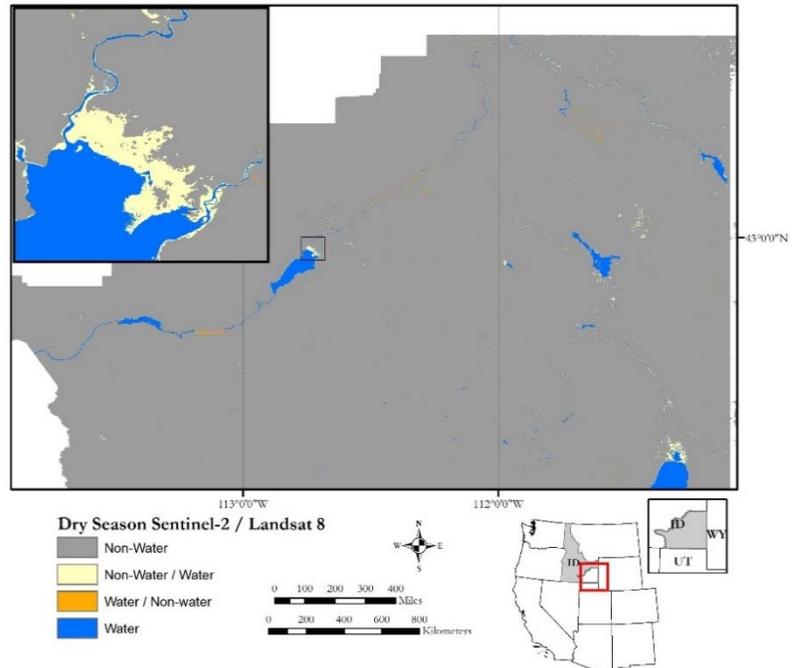
Figure 7. Comparison of Sentinel-2 imagery and Landsat 8 imagery captured during the month of August in 2016 after all of the snowpack has melted and has mostly infiltrated into groundwater reserves.

can account for platform disagreement when the disagreement does not cover a large spatial extent and is located around agreed upon water bodies. The differences across platforms could also be the result of the differences between the wavelengths covered by the NIR band in Sentinel-2 and Landsat 8 platforms. Mandanici and Bitelli (2016) found that Landsat 8's near-infrared (NIR) band most closely correlates with Sentinel-2s' red edge band over the larger NIR wavelength. Therefore, it may be helpful to adopt band 8a, red edge, instead of band 8, NIR, currently used in the SWIM model. Unfortunately the red edge band increases the bands spatial resolution from 10 meters to 20 meters and this is the reason the original NIR was used in this study. Previous research also found that correlations are decreased between NDWI calculated with each platform in calm water, most likely dues to low reflectance of water which increases the signal-to-noise ratio (Mandanici and Bitelli, 2016). However, it is likely that turbid water sources were more likely to cause agreeance across platforms because turbidity produces higher and more homogeneous reflectance values (Mandanici and Bitelli, 2016). Disagreement can also be caused by temporal collection differences. The dates chosen for Sentinal-2 and Landsat 8 imagery were limited by cloud cover and caused collection dates across platforms to differ by up-to a week. It is well known, that a sensors' recorded signal is dependent on the radiance coming from the surface and atmospheric effects. A longer time step between the acquisitions may increase the differences in radiometry because of differences in atmosphere and surface reflection conditions. Overall, the Sentinal-2 data was better at picking up the smaller details of rivers and streams while defining larger water bodies and its outlets. Landsat 8 data on the other hand seemed to be able to differentiate possible water sites a little better.
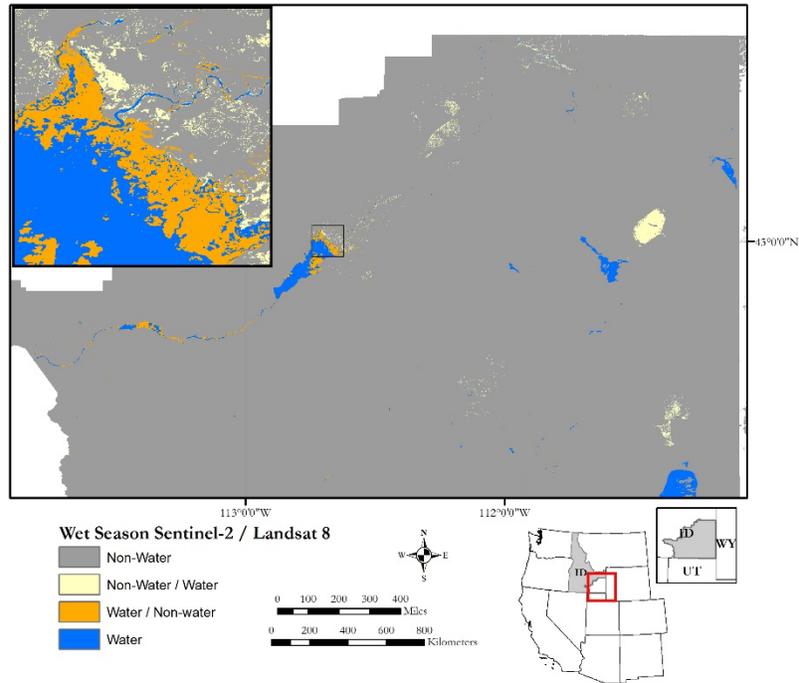
Figure 8. Comparison of Sentinel-2 imagery and Landsat 8 imagery captured during the month of July in 2016 when snowpack, the main source of surface water in Idaho, is melting.

4.5 Future Work

Stream and river fragmentation were prevalent throughout all of the classifications. This is because many of the streams and rivers in Southeast Idaho are relatively small and do not reflect enough radiance even at 10 meter pixel resolution. In order to correct this issue, an inclusion of a path-tracking algorithm can be applied to reduce fragmentation and produce continuity of the streams. Furthermore, using higher resolution imagery, such as WorldView 3 at 1.24 m spatial resolution, may also be beneficial for a more accurate detection of these water bodies. Additionally, the same methodologies can be used in a study area outside of Southeast Idaho, expanding to test water identification outside the semiarid high desert environment.

5. Conclusions

This project successfully created a Surface Water Indication Model in both GEE and ArcMap. A Support Vector Machine (SVM) classified the water indices, topographic data, and secondary variables. The water indices were comprised of the AWEsh, MNDWI, SAVI, MBSRV, MBSRN, and iron ratio equations, as well as the thermal band (B10), which was derived using Landsat 8 Operational Land Imager (OLI) Thermal Infrared Sensor (TIRS). Topographic information, consisting of slope, aspect, and elevation, was extracted from the Shuttle Radar Topography Mission (SRTM). The SVM was trained with over 500 training pixels per class to produce data layers with six cover classes: basalt, open water, dark vegetation, urban, sporadic vegetation/bare soil, and mixed water. Leveraging several water indices, instead of just one, enabled the classifier to better predict and identify water. Error matrices showed that classification accuracy for the water class was 80%. However, distinguishing between non-water classes proved difficult for the classifier. This may indicate that SWIM-GEE's performance could be better improved by including non-water thresholds within the model.

6. Acknowledgments

7. Glossary

Closed Canopy - created as a class to highlight areas that may be obscuring water signatures, for instance when a forest canopy completely covers a stream. So when an area is classified at "Closed Canopy" it could indicated water is nearby, unless of course it is covering a hilltop rather than a draw.

Exposed Substrate- excludes soil, but includes exposed solid rock and features like gravel that is found mixed throughout all sagebrush steppe habitat. So when you look at this confusion matrix "10" of the validation checks that were visually look like sagebrush steppe may have actually been classified correctly as exposed substrate

Indices – remote sensing-derived indexes

Intermittent – water body that normally ceases flowing or dry up for months in a year

MODIS – MODerate resolution Imaging Spectroradiometer: instrument that captures data in 36 bands onboard Terra Satellite.

Moraine – A mass of rocks and sediment carried down and deposited by a glacier, typically as ridges at its edges or extremity

Open Water - easily detected water

Perennial – water body that keeps full or flowing all year or most of the year

Raster – made up of matrix cells that contain value; are organized in row and columns

Sagebrush Steppe or Soil - this represents bare earth or vegetation that is sparse which indicates a lack of available water

Urban - are areas like buildings or large parking areas

Vector – data representation of world features in points, lines, and polygons

8. References

Bauer, M. E., Biehl L. L., Robinson B. F. (1980) Final Report Volume 1: Field Research on the Spectral Properties of Crops and Soils. NASA Rep. SR-PO-O4022. Laboratory for Applications of Remote Sensing. West Lafayette, IN.

Berk. (2009, November 6). Classification and Regression Trees. Data Mining with Rattle and R: The Art of Excavating Data for Knowledge Discovery. *Use R*, pp. 36-350. Retrieved from http://doi.org/10.1007/s00038-011-0315-z

Breiman, L., Friedman, J., Stone, C. J., & Olshen, R. A. (1984). Classification and regression trees. CRC press.Burges, C. J. C. (1998). A Tutorial on Support Vector Machines for Pattern Recognition. Data Mining and Knowledge Discovery, 2(2), 121–167. http://doi.org/10.1023/A:1009715923555

Cafarella, M., Chang, E., Fikes, A., Halevy, A., Hsieh, W., Lerner, A., Madhavan, J., Muthukrishnan, S. (2008). Data management projects at Google. ACM SIGMOD Record, 37(1), 34–38. http://doi.org/10.1145/1374780.1374789

Cortes, C., Vapnik V. (1995, March 8). Support Vector Networks. Machine Learning. Retrieved from http://link.springer.com/10.1007/BF00994018

Donchyts, G., Schellekens, J., Winsemius, H., Eisemann, E., & Van de Giesen, N. (2016). A 30 m Resolution Surface Water Mask Including Estimation of Positional and Thematic Differences Using Landsat 8, SRTM and OpenStreetMap: A Case Study in the Murray-Darling Basin, Australia. *Remote Sensing, 8*, 386. Retrieved from http://doi.org/10.3390/rs8050386

Feyisa, G. L., Meilby, H., Fensholt, R., & Proud, S. R. (2014). Remote Sensing of Environment Automated Water Extraction Index: A new technique for surface water mapping using Landsat imagery. *Remote Sensing of Environment, 140*, 23-35.

Irons, James R. (2016, November). The Worldwide Reference System. NASA. Retrieved from http://landsat.gsfc.nasa.gov/the-worldwide-reference-system/

Jawak, Jawak, S. D., Kulkarni, K., & Luis, A. J. (2015). A Review on Extraction of Lakes from Remotely Sensed Optical Satellite Data with a Special Focus on Cryospheric Lakes. *Advances in Remote Sensing, 04(03)*, 196–213. Retrieved from http://doi.org/10.4236/ars.2015.43016

Jin, S., Homer, C., Yang, L., Xian, G., Fry, J., Danielson, P., & Townsend, P. A. (2013). Automated cloud and shadow detection and filling using two-date Landsat imagery in the USA. *International Journal of Remote Sensing, 34(5)*, 1540–1560. Retrieved from http://doi.org/10.1080/01431161.2012.720045

Jones, J. W., & Starbuck, M. J. (2015). *USGS.gov.* Retrieved from Dynamic Surface Water Extent (DSWE): http://remotesensing.usgs.gov/ecv/document/dswe_algorithm_description.pdf

Mandanici E., & Bitelli G. (2016). Preliminary Comparison of Sentinel-2 and Landsat 8 Imagery for a Combined Use. *Remote Sensing,* 8 (1014) 1-10. doi:10.3390/rs8121014

McFeeters, S. K. (2013). Using the Normalized Difference Water Index (NDWI) within a Geographic Information System to Detect Swimming Pools for Mosquito Abatement: A Practical Approach. *Remote Sensing, 5(7)*, 3544-3561. Retrieved from http://doi.org/10.3390/rs5073544

NASA JPL. (2013). NASA Shuttle Radar Topography Mission Global 1 arc second [Data set]. NASA LP DAAC. https://doi.org/10.5067/MEaSUREs/SRTM/SRTMGL1.003

Saraswat, M. (2016, April 12). A Complete Tutorial on Tree Based Modeling from Scratch (in R & Python). Retrieved from https://www.analyticsvidhya.com/blog/2016/04/complete-tutorial-tree-based-modeling-scratch-in-python/

U.S. Fish and Wildlife Service. (2002). *National wetlands inventory: A strategy for the 21st century.* Washington, DC: U.S. Department of the Interior, Fish and Wildlife Service.

U.S. Geological Survey (2014). Provisional Landsat 8 OLI (Operational Land Imager) Surface Reflectance [Data set]. U.S. Geological Survey; Long Term Ecological Research Network. https://doi.org/10.5066/F78S4MZJ

Wright, C., & Gallant, A. (2007). Improved wetland remote sensing in Yellowstone National Park using classification trees to combine TM imagery and ancillary environmental data. *Remote Sensing of Environment, 107*, 582-605.

Xu, H. (2006). Modification of Normalized Difference Water Index (NDWI) to Enhance Open Water Features in Remotely Sensed Imagery. *International Journal of Remote Sensing, 27(14)*, 3025-3033. Retrieved from http://doi.org/10.1080/01431160600589179

9. Appendices
9.1 Dynamic Surface Water Extent
9.1.1 SWIM results versus the USGS Dynamic Surface Water Extent product (DSWE)
The U.S. Geological Survey (USGS) is in the process of creating the Dynamic Surface Water Extent (DSWE) product with the aim of providing increased spatial and temporal monitoring of the dynamics of non-ocean surface water extents (Jones & Starbuck, 2015). These products are being produced to include the entire archived and currently available Landsat imagery. An early look at water indices, as well as the provisional Dynamic Surface Water Extent (DSWE) from the U.S. Geological Survey, did seem to indicate that basaltic rock often gave false water signatures (Jones & Starbuck, 2015). This could be problematic, since it is common to find large basalt formations and smaller rock outcrops in southeastern Idaho. The provisional data DSWE products that matched the project's study area and period were compared with the results produced by the SWIM tool. While the study area is just partially in path 39 and row 30, the full Landsat scene was included during the comparison in order to maximize the evaluation. Prior to comparison, an agriculture mask produced from the 2011 National Land Cover Dataset (NLCD) was applied to the SWIM-GEE results in such a way that when the two results were compared the mask was also applied to the DSWE results. After this mask was applied, the SWIM-GEE no water, open water, and mixed water classes were compared to the four classes produced in DSWE, no water, high confidence of water, moderate confidence of water, and partial surface water. The classes for each of these results were generalized, so when a pixel was not classified the same between the two results, areas classified with a high confidence level or said to be partial water were shown as water. The USGS is also responsible for the National Hydrography Dataset (NHD) which was also used to compare with the SWIM results.
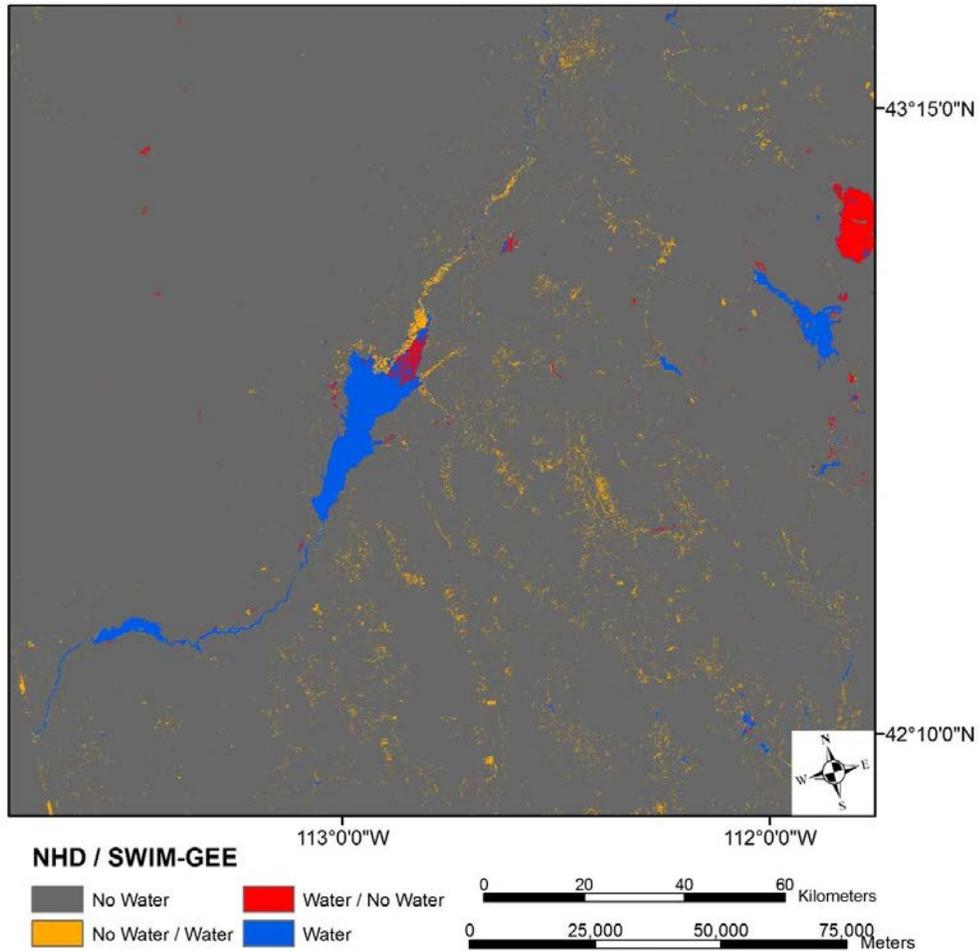
Figure 9. The SWIM-GEE results were compared to the NHD product for the full project extent with an agriculture mask applied. The figure displays pixels that were classified as water by the SWIM-ArcGIS and non-water as SWIM-GEE in red; orange shows pixels that SWIM-ArcGIS classified non-water and SWIM-GEE classified as water pixels; areas where both models classified pixels as non-water are shown in gray and water in blue.

The total disagreement, 19.34%, for the NHD-SWIM comparison is the highest seen out of the three comparisons performed in this project. This disagreement does have founding when visual checks are completed on areas NHD has identified as water and SWIM-GEE does not (purple of Figure 13). However, some of the disagreements could be explained with differences in boundaries. For instance, the NHD does have a riparian areas identified in its database (blue circle Figure 13), however, it is shown in red in Figure 13. This is, most likely because SWIM identified a greater boundary than the boundary recorded in NHD.

Table 4. Summary of the areas (km²) compared between NHD and SWIM classes.

| | Area | |
NHD / SWIM-GEE	Square kilometer	Percentage
No Water	34,053	79%
No Water / Water	8,162	19%

Water / No Water	201	0%
Water	820	2%
Total Agreement	34,873	81%
Total Disagreement	8,363	19%

9.1.2 SWIM results versus an initial DSWE product

As shown in Table 4 most of the 4.99% disagreement between DSWE and SWIM-GEE was due to DSWE classifying basalt as water and SWIM-GEE classifying non-water as water, where 2.15 % of the 2.54% of the "No Water / Water" comparison is due to partial water classification rather than open water.
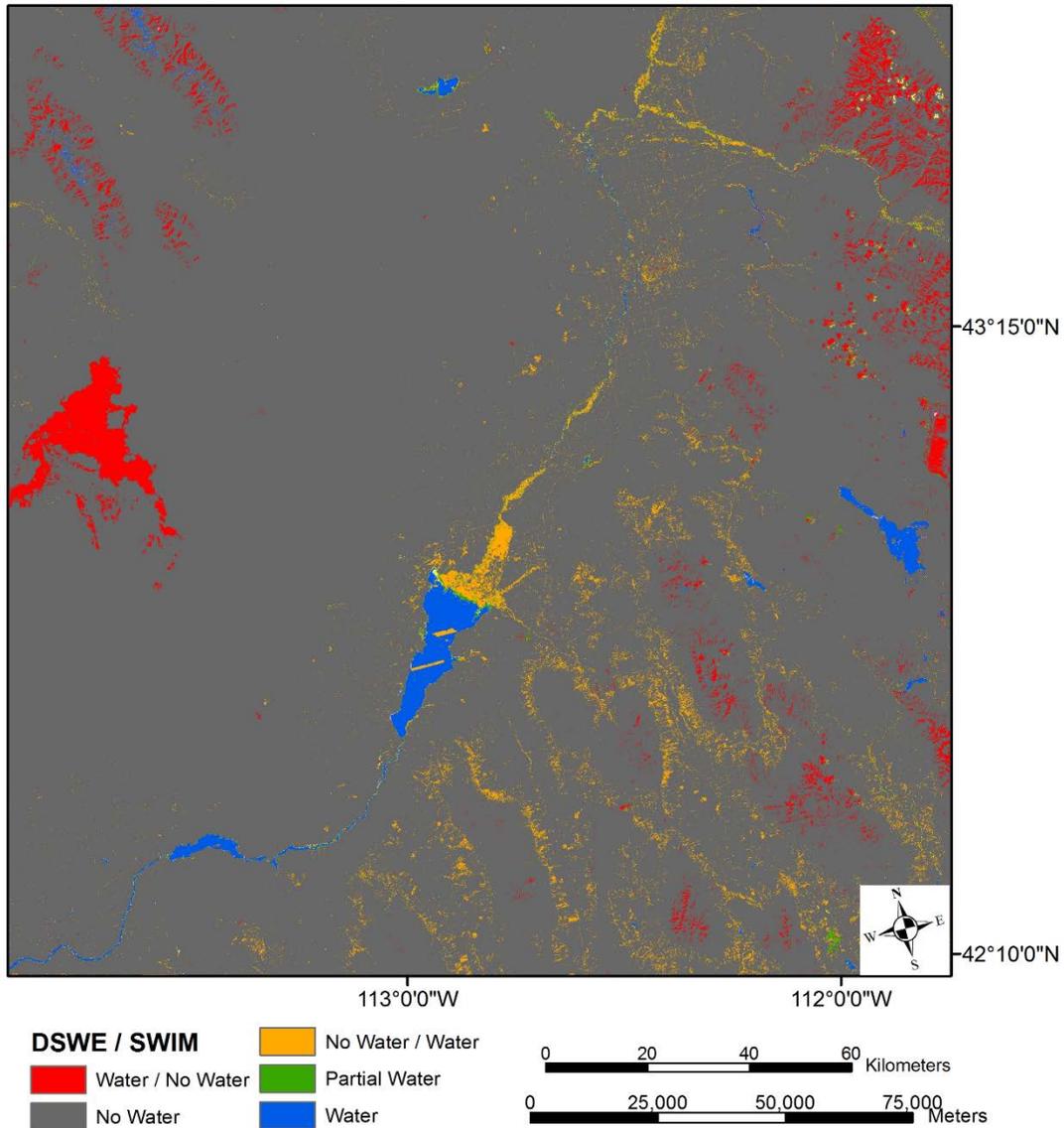
Figure 10. *The SWIM-GEE results were compared to the DSWE product for the Landsat scene 39/30 (path/row) and an agriculture mask was applied. The figure displays pixels that were classified as water with DSWE and non-water with SWIM-GEE (red); pixels that DSWE classified as non-water but SWIM-GEE classified as water (orange); and areas that both models classified as non-water (gray), partial water (green), and water (blue).*

Table 5 *Summary of the areas (km²) compared between DSWE and SWIM classes.*

DSWE / SWIM	Area	
	KM²	Percent
Water / No water	872	2%
No Water / Water	900	3%
Partial Water	75	0%
Water	398	1%
No Water	3,3251	94%
Total Agreeance	3,3724	95%
Total Disagreement	1,772	5%

9.2 Error Matrices

Table 6. *Error Matrix for the first out of three classifications completed and accuracy calculated in GEE.*

Classes	Basalt	Open Water	Dark Vegetation	Urban	Bare Soil/ Sporadic Vegetation	Mixed Water	**Accuracy**
Basalt	159	0	2	0	3	10	91%
Open Water	0	190	0	0	0	4	98%
Dark Vegetation	5	2	151	0	6	12	86%
Urban	9	0	1	117	8	41	66%
Bare Soil / Sporadic Vegetation	2	0	10	15	135	4	81%
Mixed Water	12	1	14	10	1	132	78%
Accuracy	85%	98%	85%	82%	88%	65%	**84%**

Table 7. *Error Matrix for the second out of three classifications completed and accuracy calculated in GEE.*

Classes	Basalt	Open Water	Dark Vegetation	Urban	Bare Soil/ Sporadic Vegetation	Mixed Water	**Accuracy**
Basalt	141	0	3	3	1	2	94%
Open Water	0	159	0	0	0	1	99%
Dark Vegetation	6	2	156	1	6	5	89%
Urban	11	0	0	137	18	9	78%
Bare Soil / Sporadic Vegetation	8	0	14	3	130	0	84%
Mixed Water	6	21	23	24	6	97	55%
Accuracy	82%	87%	80%	82%	81%	85%	**83%**

Table 8. *Error Matrix for the third out of three classifications completed and accuracy calculated in GEE.*

Classes	Basalt	Open Water	Dark Vegetation	Urban	Bare Soil/ Sporadic Vegetation	Mixed Water	**Accuracy**
Basalt	141	0	7	0	7	2	90%
Open Water	0	161	0	0	0	2	99%
Dark Vegetation	2	1	157	0	4	16	87%
Urban	19	0	1	128	4	35	68%
Bare Soil / Sporadic Vegetation	2	1	11	16	135	3	80%
Mixed Water	6	7	26	18	2	124	68%
Accuracy	83%	95%	78%	79%	89%	68%	**82%**

Table 9. *Error Matrix for the first out of three classifications completed in GEE and accuracy calculated in ArcMap.*

Classes	Basalt	Open Water	Dark Vegetation	Urban	Bare Soil/ Sporadic Vegetation	Mixed Water	**Accuracy**
Basalt	159	0	2	0	3	10	91%
Open Water	0	190	0	0	0	4	98%
Dark Vegetation	5	2	151	0	6	12	86%
Urban	9	0	1	117	8	41	66%
Bare Soil / Sporadic Vegetation	2	0	10	15	135	4	81%
Mixed Water	12	1	14	10	1	132	78%
Accuracy	85%	98%	85%	82%	88%	65%	**84%**

Table 10. *Error Matrix for the second out of three classifications completed in GEE and accuracy calculated in ArcMap.*

Classes	Basalt	Open Water	Dark Vegetation	Urban	Bare Soil/ Sporadic Vegetation	Mixed Water	**Accuracy**
Basalt	141	0	3	3	1	2	94%
Open Water	0	159	0	0	0	1	99%
Dark Vegetation	6	2	156	1	6	5	89%
Urban	11	0	0	137	18	9	78%
Bare Soil / Sporadic Vegetation	8	0	14	3	130	0	84%
Mixed Water	6	21	23	24	6	97	55%
Accuracy	82%	87%	80%	82%	81%	85%	**83%**

Table 11. *Error Matrix for the third out of three classifications completed in GEE and accuracy calculated in ArcMap.*

Classes	Basalt	Open Water	Dark	Urban	Bare Soil/	Mixed	**Accuracy**

			Vegetation		Sporadic Vegetation	Water	
Basalt	141	0	7	0	7	2	90%
Open Water	0	161	0	0	0	2	99%
Dark Vegetation	2	1	157	0	4	16	87%
Urban	19	0	1	128	4	35	68%
Bare Soil / Sporadic Vegetation	2	1	11	16	135	3	80%
Mixed Water	6	7	26	18	2	124	68%
Accuracy	83%	95%	78%	79%	89%	68%	**82%**